Visualization of vitamin A metabolism

Koenders, S.T.A.

Chapter 4

Biological Evaluation of LEI-945

Published as part of S.T.A. Koenders *et al., ACS Cent. Sci.*, **5**, 1965-1974 (2019).

Introduction

Aldehyde dehydrogenases (ALDHs) perform an important role in cellular metabolism by converting aldehydes into carboxylic acids, some of which perform important biological roles, such as retinoic acid.[1] Aldehydes are intrinsically reactive and may bind to DNA or proteins, resulting in cellular damage. A buildup of these metabolites in the cell is toxic.[2] Fast conversion of such compounds into less toxic and easily excreted carboxylic acid metabolites is therefore essential for cell survival and proliferation. The human ALDH family consists of 19 enzymes, each with its own preferred type of substrates and covering a wide range of endogenous and exogenous aldehydes.[3,4]

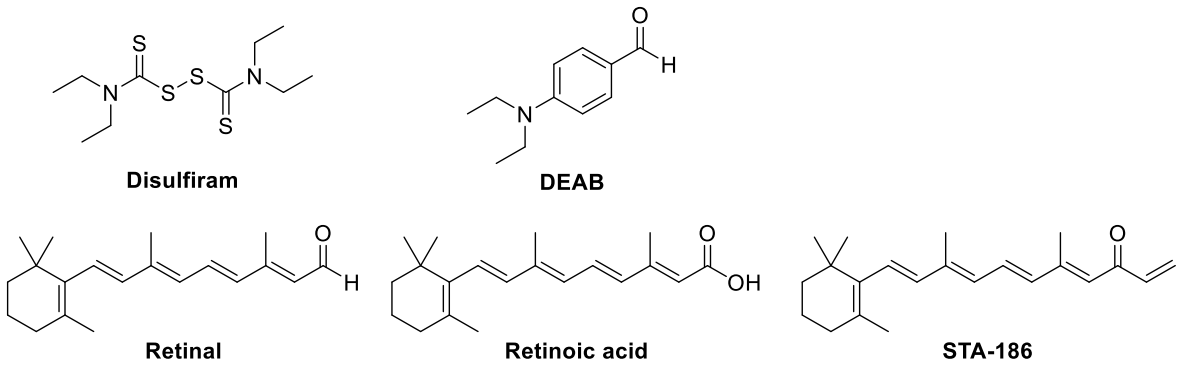

Fig. 4.1 | Chemical structures of ALDH inhibitors and retinoids used in this chapter

Three ALDHs (ALDH1A1, ALDH1A2, ALDH1A3) have been shown to convert retinal into retinoic acid and are therefore classified as retinaldehyde dehydrogenases.[3,4] Retinoic acid regulates many cellular and physiological functions. Enabling a specific readout of the activity of these enzymes would allow researchers to study the individual contribution of these enzymes to processes such as embryonic development, immunomodulation, neuronal differentiation and (cancer) stem cell proliferation.[5-8]

Chapter 3 described the design and synthesis of the first-in-class retinal based probe **LEI-945** for the profiling of retinaldehyde dehydrogenases. In this chapter the biological evaluation of activity-based probe (ABP) **LEI-945** is reported.

Results and discussion

LC-UV/MS based assay for in situ retinal conversion

Most biochemical ALDH assays described in literature rely on the change in absorbance of nicotinamide adenine dinucleotide (NAD^+) upon conversion into NADH, which is produced during enzymatic aldehyde dehydrogenation. However, the catalytic cysteine of ALDHs can be easily oxidized in non-cellular environments. To overcome this problem these *in vitro* assays rely on the addition of reducing agents, such as dithiothreitol or tris(2-carboxyethyl)phosphine, to keep the cysteine in its reduced and catalytically active state. Often *in vitro* assays are also performed in buffers with a pH of ≥ 8.0, further increasing the reactivity of the cysteine. As these assay conditions do not resemble physiologically relevant conditions, there is a need for a cellular assay that reports directly on the formation of retinoic acid by ALDH enzymes.

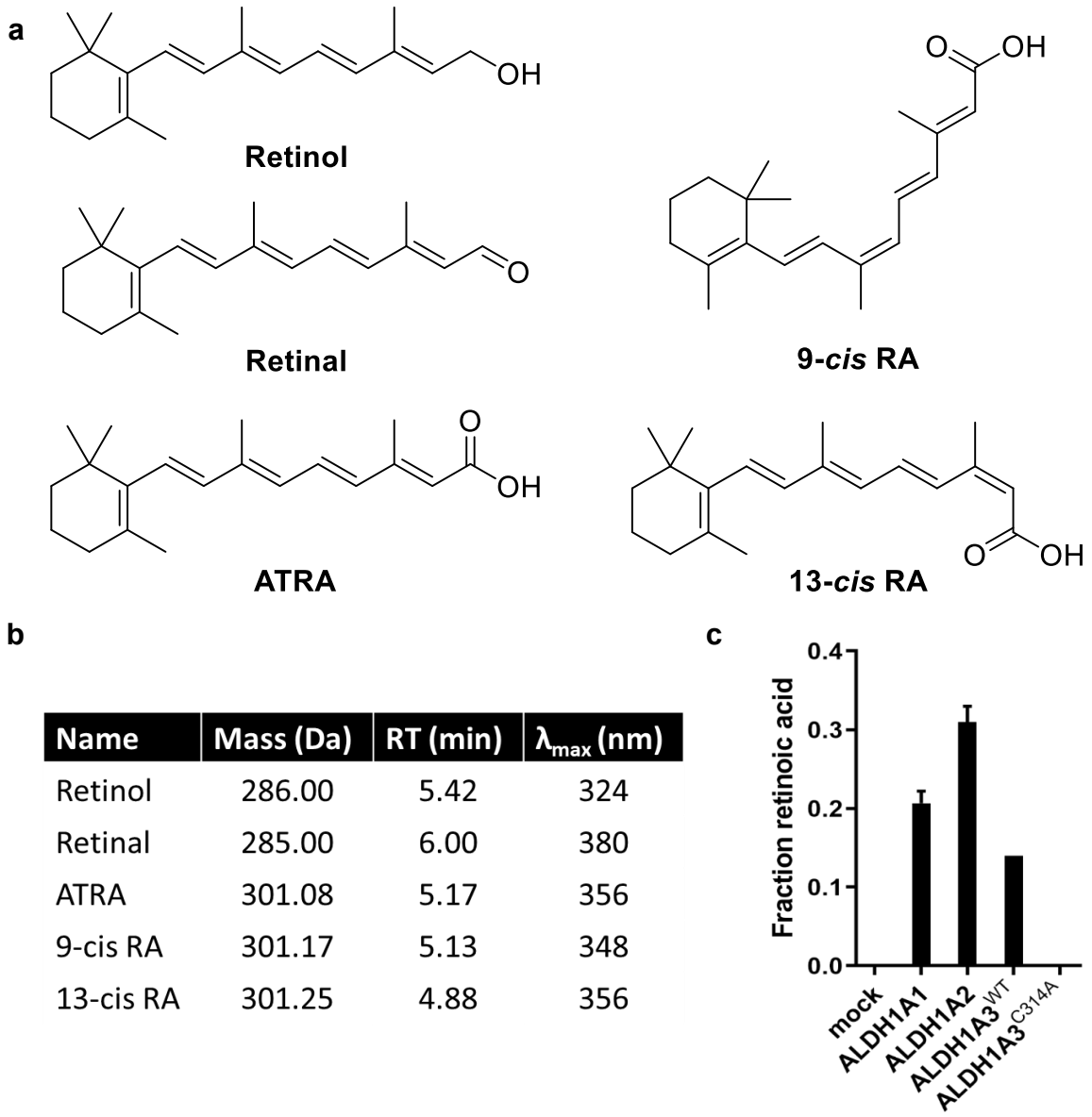

Name	Mass (Da)	RT (min)	λ_{max} (nm)
Retinol	286.00	5.42	324
Retinal	285.00	6.00	380
ATRA	301.08	5.17	356
9-cis RA	301.17	5.13	348
13-cis RA	301.25	4.88	356

Fig. 4.2 | Chemical structures of retinoid standards and data from *in situ* retinal conversion assay. a, Chemical structures of retinoid standards. **b,** Detected values for each of the retinoid standards, detected mass, retention time (RT) and wavelength maximum (λ_{max}). **c,** Retinoic acid production by U2OS cells overexpressing ALDHs. Data represent mean values ± SD; $N = 3$ biological replicates measured twice.

To determine whether recombinant ALDH enzymes are active and capable of converting retinal, an *in situ* substrate assay was developed. It was envisioned that a LC-UV/MS-based method could be established to measure the cellular conversion of retinal into retinoic acid. First, the retention time and maximum wavelength (λ_{max}) of retinoid standards were measured on a LC-UV/MS using a gradient of 10% acetonitrile for 1.5 minutes followed by 90% acetonitrile for 7.5 minutes (**Supplementary Fig. 4.1**).

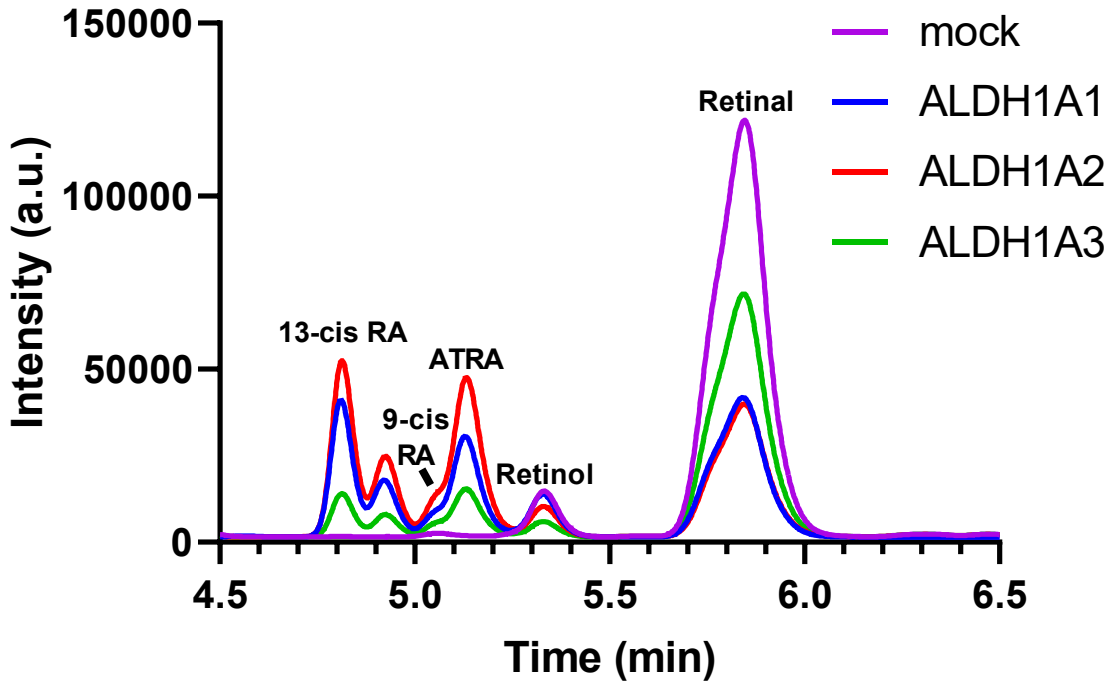

Fig. 4.3 | *In situ* retinal conversion assay using LC-UV/MS. Overlay of UV traces for mock, ALDH1A1, ALDH1A2 and ALDH1A3 overexpressed in U2OS cells.

The λ_{max} values were 324, 380, 356, 348 and 356 nm for retinol, retinal, all-*trans*-retinoic acid (ATRA), 9-*cis* RA and 13-*cis* RA, respectively (**Fig. 4.2b**). This is consistent with reported values in ethanol.[9] A calibration curve was made using a mixture of the five standards which was measured at 324, 356 and 380 nm. The retention times of the retinoid standards were 5.42, 6.00, 5.17, 5.13 and 4.88 minutes, respectively (**Fig. 4.2b**). The MS data were used to confirm the correct assignment of the peaks (**Fig. 4.2b**).

ALDH1A1, 1A2 and 1A3 were transiently overexpressed in U2OS human osteosarcoma cells. This cell line was used as it showed no endogenous conversion of retinal. Two days after transfection, cells were treated with retinal (30 µM, 4 h) in medium with serum. Cells were then lysed with acetonitrile. Insoluble compounds were removed by centrifugation. The samples were concentrated, dissolved in LC-MS sample solution and measured using the protocol previously described. An overlay of the UV traces for ALDH1A1, 1A2, 1A3 is shown in **Fig. 4.3**.

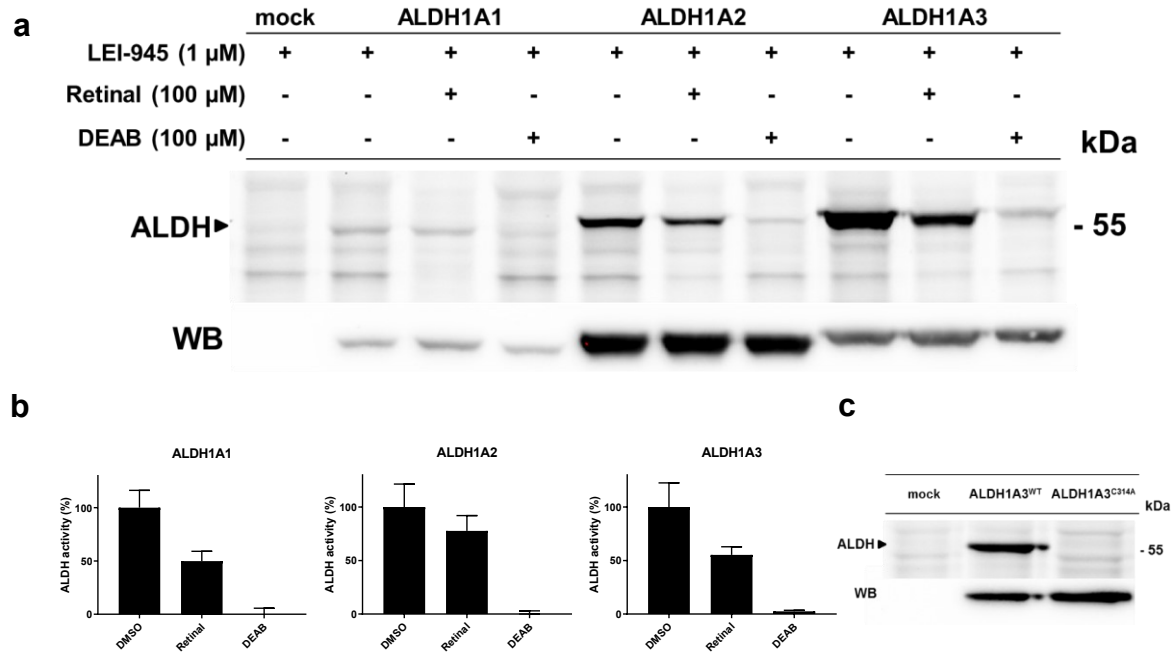

Fig. 4.4 | *In situ* labeling of ALDH by LEI-945 and competition with the natural substrate and pan-ALDH inhibitor DEAB. a, *In situ* labeling of ALDH1A1, ALDH1A2, ALDH1A3 transiently transfected in U2OS cells using **LEI-945** (1 µM) for 1 h at 37 °C. Competition was performed with natural substrate retinal (100 µM) or general ALDH inhibitor DEAB (100 µM). **b**, Competition of **LEI-945** labeling of overexpressed ALDH enzymes in U2OS cells. Data represent mean values ± SD; $N = 3$ experiments per group (biological replicates). **c**, *In situ* labeling of ALDH1A3^{WT} and mutant ALDH1A3^{C314A} with **LEI-945** (1 µM) for 1 h at 37 °C.

Formation of ATRA and its *cis*-isomers is clearly catalyzed by all three ALDH isozymes. An additional peak is detected at 4.92 minutes with the same mass as retinoic acid, probably corresponding with 11-*cis* retinoic acid. Overexpression of ALDH1A3^{C314} in U2OS confirmed that Cys314 was required for the enzymatic activity of ALDH1A3 (**Fig. 4.2c**). These data show that recombinant ALDH1A1, ALDH1A2 and ALDH1A3 are active and can be used to establish whether **LEI-945** acts as an activity-based probe for retinaldehyde dehydrogenases.

LEI-945 reacts with overexpressed ALDHs in situ to form a covalent adduct

To assess whether **LEI-945** acts as a retinaldehyde dehydrogenase ABP, pcDNA3.1 plasmids containing either recombinant human ALDH1A1, ALDH1A2 or ALDH1A3 fused to a FLAG-tag were transiently transfected in U2OS cells. Living cells were treated with **LEI-945** (1 µM) in serum free medium for 1 hour, lysed and the probe labelled proteins ligated with Alexa Fluor 647 dye under copper(I)-catalysed azide-alkyne [2+3] cycloaddition conditions.

The protein samples were resolved by sodium dodecyl sulphate polyacrylamide gel electrophoresis (SDS-PAGE) and visualized by in-gel fluorescent scanning. A fluorescent band at 55 kDa was apparent in samples harvested from all three transfected cell cultures, but not in the mock-treated cells (**Fig. 4.4a**). All fluorescent bands were at the same height as the signal generated by an α-FLAG antibody in a separate Western blotting experiment. This molecular weight matches with that of the transfected retinaldehyde dehydrogenases, suggesting that **LEI-945** indeed reacted with these proteins in a covalent manner. Fluorescent labeling intensity was reduced by pretreatment with retinal (100 μM) as well as with the general ALDH inhibitor, DEAB (100 μM) (**Fig. 4.4a,b**).[10]

Site-directed mutagenesis of the catalytic Cys314 into alanine in ALDH1A3, which was chosen as a representative retinaldehyde dehydrogenase, abolished labeling of the enzyme with **LEI-945**, whereas protein expression was not affected as determined by an α-FLAG antibody (**Fig. 4.4c**). Altogether, these data demonstrate that **LEI-945** can efficiently label ALDH1A1, ALDH1A2 and ALDH1A3 in an activity-dependent manner by forming a covalent and irreversible bond with the catalytic cysteine thiol.

Mapping of endogenous ALDHs in A549 lung cancer cells using LEI-945

To establish the potential of **LEI-945** to detect endogenous retinaldehyde dehydrogenases, non-small-cell lung cancer cell line A549, known to express ALDH1A1[11,12], was incubated with **LEI-945**. This yielded a fluorescent band at around 55 kDa, which could be significantly and dose-dependently reduced by preincubation with either DEAB, retinal, disulfiram or **STA-186**, with pIC_{50} values in the range of 5.0-5.9 (**Fig. 4.5**).

To find out which proteins are irreversibly and covalently labelled by **LEI-945**, a label-free chemical proteomics experiment was performed. **LEI-945** (1 μM, 1 h)-treated A549 cells were lysed and reacted with biotin-N_3, after which probe-labelled proteins were enriched for by streptavidin bead pull-down. Subsequent tryptic digestion, protein identification and quantification by mass spectrometry resulted in the identification 34 significantly enriched proteins, including ALDH1A1, ALDH2, ALDH3A2 and ALDH3B1 (**Fig. 4.6a,b**, **Supplementary Table 1**).

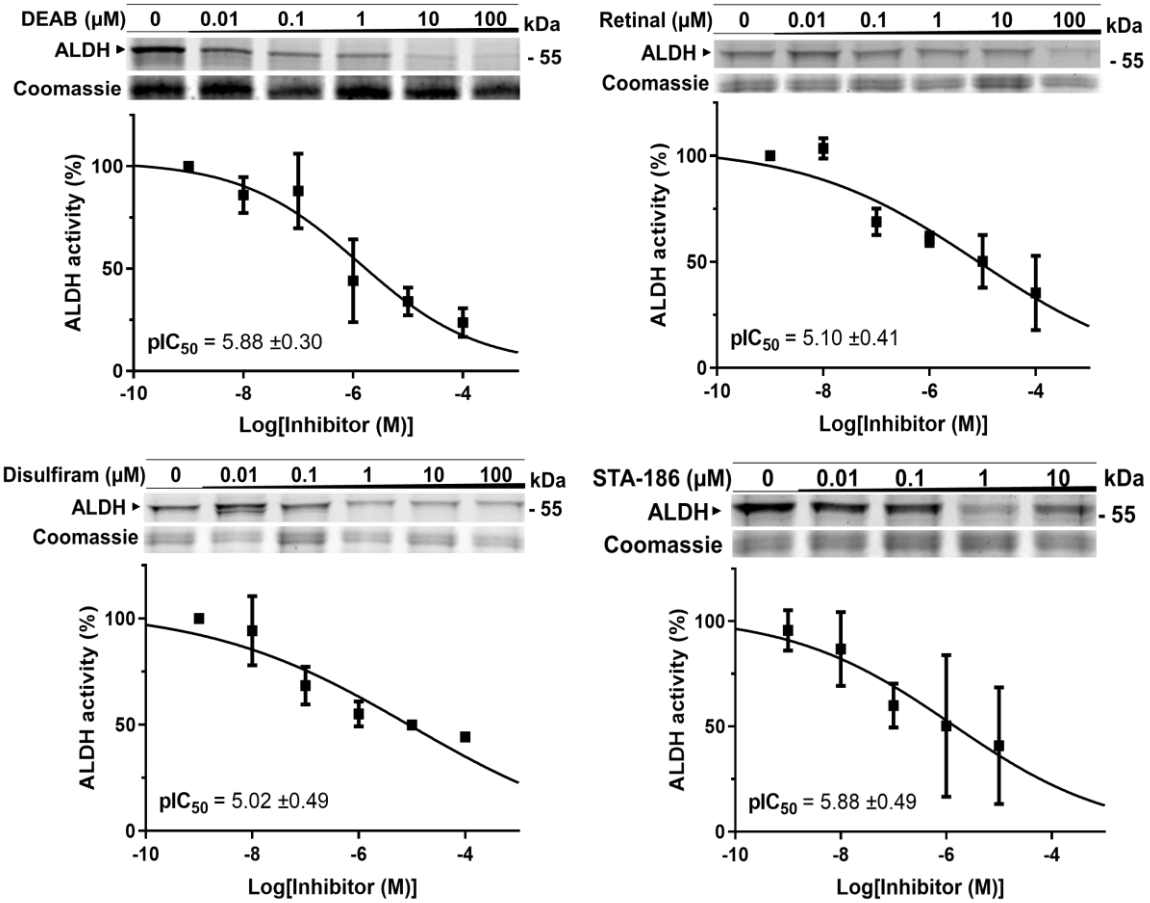

Fig. 4.5 | *In situ* labeling of endogenous ALDHs by LEI-945 and competition with natural substrate and inhibitors. *In situ* labeling of endogenous ALDH enzymes in A549 lung cancer cells with **LEI-945** (1 μM) and competition with ALDH inhibitors or natural substrate. Graphs showing the pIC_{50} values ± SD of several ALDH inhibitors as determined by competitive ABPP with probe **LEI-945** (1 μM). Data represent mean values ± SD; $N = 3$ experiments per group (biological replicates).

To exclude the possibility that the warhead covalently binds to reactive cysteines irrespective of recognition based on the retinal scaffold, the list of 34 proteins significantly enriched by **LEI-945** was compared with a list of the 150 most reactive cysteines. This list was compiled by Cravatt *et al.*[13] using ABPP with the reactive nucleophile iodoacetamide in MDA-MB-231, MCF7 and Jurkat cancer cell lines. Only two proteins (ALDH2 and RTN3) from this list were identified as interacting partners of **LEI-945**. This suggested that the scaffold of **LEI-945** confers selectivity to its binding partners and does not randomly label proteins with hyper reactive cysteines.

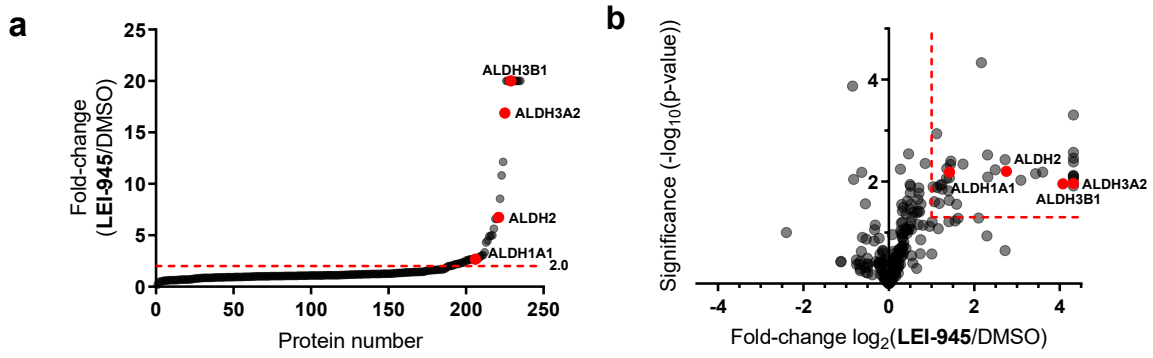

Fig. 4.6 | ABPP of ALDHs in A549 cells. a, Fold-change (**LEI-945**/DMSO) plot for total proteins identified in chemical proteomics experiment with probe **LEI-945** (1 μM). Red lines indicate the threshold fold-change of 2-fold enrichment and the maximum fold-change is set at 20. Red dots represent significantly enriched ALDH enzymes. **b**, Volcano plot for total proteins identified in chemical proteomics experiment with probe **LEI-945** (1 μM). Red lines indicate threshold values (fold-change > 2; p-value < 0.05) marking significantly enriched proteins. Red dots represent significantly enriched ALDH enzymes. For parts **a** and **b**, data are from $N = 4$ experiments (biological replicates).

Some of the proteins found, have been previously reported to interact with retinoids and related lipids, such as sarcoplasmatic/endoplasmic reticulum calcium ATPase 2 (ATP2A2), ADP/ATP translocase 2 (SLC25A5), ADP/ATP translocase 3 (SLC25A6), voltage-dependent anion-selective channel protein 2 (VDAC2) and voltage-dependent anion-selective channel protein 3 (VDAC3).[14–17]

Pathway analysis using the KEGG[18], UniProt[19] and PANTHER[20] databases and DAVID[21] analytic tools, revealed that most enzymes and transporters are located in the endoplasmic reticulum and mitochondria (**Fig. 4.7a**). Many proteins involved in fatty acid degradation, β-alanine and histidine metabolism were enriched, which is in line with the proposed role of ALDH enzymes in these cellular pathways (**Fig. 4.7b**).[3]

A significant number of unannotated proteins were found, which may be involved in retinal/retinoic acid biochemistry and biology (**Fig. 4.7c**). To investigate whether these proteins are also targeted by retinal and DEAB, a competitive chemical proteomics experiment was performed (**Fig. 4.7d**). Retinal inhibited over 85% of the targets of **LEI-945**, including all identified ALDH enzymes apart from ALDH2, whereas DEAB was much more selective and reduced the labeling of only three proteins (ALDH1A1, ALDH2 and PCNA-interacting partner (PARPBP)).

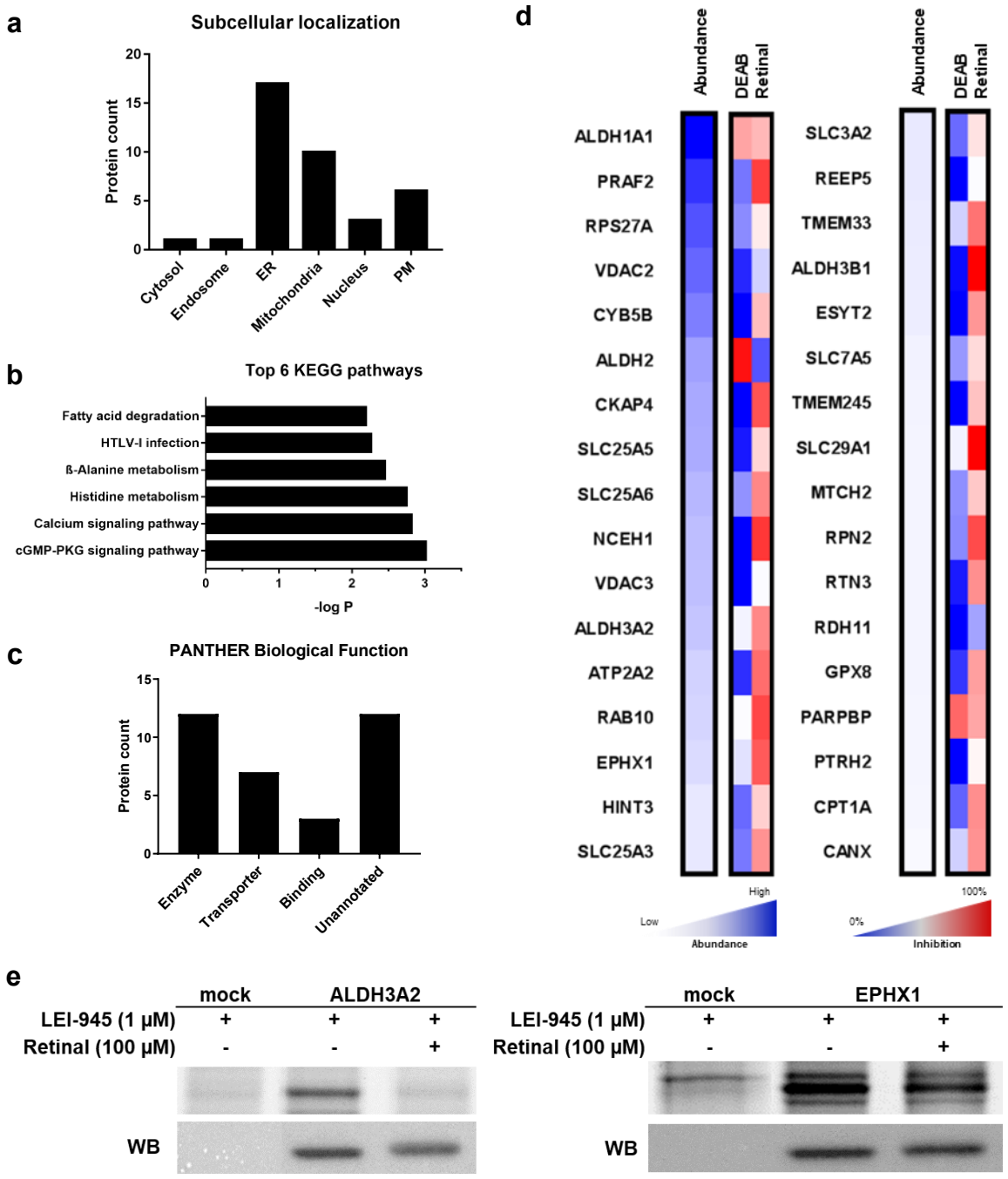

Fig. 4.7 | Proteomics data of retinal interacting proteins in A549 cells. a, Subcellular localization of significantly enriched proteins as annotated by the UniProt database. **b**, Top 6 pathways enriched in the group of significantly enriched proteins as determined by screening on the KEGG database. **c**, Biological functions annotated to significantly enriched proteins by the PANTHER database. **d**, Maximum abundance (white = low; blue = high) and inhibition (blue = 0%; red = 100%) by pan-ALDH inhibitor DEAB (100 µM) and natural substrate retinal (100 µM) in competitive ABPP experiments with **LEI-945**. Data are from $N = 4$ experiments (biological replicates). **e**, *In situ* labeling of recombinant ALDH3A2 and EPHX1 with **LEI-945** (1 µM) for 1 h at 37 °C. Competition was performed with natural substrate retinal (100 µM).

To validate the identified probe targets as retinoid-interacting proteins, we overexpressed recombinant ALDH3A2 and epoxide hydrolase 1 (EPHX1) as representative examples in U2OS cells and fluorescently labelled them with **LEI-945** (1 μM). Competition with retinal (100 μM) confirmed their ability to bind retinoids (**Fig. 4.7e**). Taken together, these data show that **LEI-945** enables the detection of various retinaldehyde dehydrogenases and other retinoid-interacting proteins in living human cells.

Conclusion

In conclusion, activity-based probe **LEI-945** was validated as the first-in-class ABP for ALDH using fluorescence and chemical proteomic approaches. **LEI-945** labelled overexpressed and endogenous retinaldehyde dehydrogenases in an activity-based fashion. Using chemical proteomics 34 proteins, including ALDH1A1, ALDH2, ALDH3A2 and ALDH3B1, have been significantly enriched from the A549 lung cancer cell line.

Acknowledgements

Hans van den Elst is kindly acknowledged for his contributions to the optimization of the LC/UV-MS assay, Hans den Dulk and Kim Wals for technical assistance with the cell culture and providing the plasmids, Pasquale Putter for determination of the *in situ* pIC_{50} values of ALDH inhibitors and Eva van Rooden for her advice on chemoproteomics and mass spectrometry analysis.

Experimental procedures

In situ labeling experiments

ALDH plasmids. For the preparation of the different constructs, full length human cDNA was purchased from Source Bioscience and cloned into mammalian expression vector pcDNA3.1, containing genes for ampicillin and neomycin resistance. ALDH1A1, ALDH1A2, ALDH1A3 and ALDH3A2 were cloned into pcDNA3.1. A FLAG-linker was cloned into the vector at the C-terminus of ALDH1A1, ALDH1A2 or ALDH1A3. EPHX1 (OHu14852D) was purchased directly from GenScript. Two step PCR mutagenesis was performed to substitute the active site cysteine for an alanine in the ALDH1A3-FLAG to obtain ALDH1A3-C314A-FLAG. All plasmids were grown in XL-10 Z-competent cells and prepped (Maxi Prep, Qiagen). The sequences were confirmed by sequence analysis at the Leiden Genome Technology Centre.

Cell culture. U2OS cells were grown in DMEM with stable glutamine and phenol red with 10% New Born Calf serum, penicillin and streptomycin at 37 °C and 7% CO_2. A549 cells were grown in DMEM with stable glutamine and phenol red with 10% New Born Calf serum, penicillin and streptomycin at 37°C and 5% CO_2. Medium was refreshed every 2-3 days and cells were passaged twice a week. Cell lines were purchased from ATCC and were regularly tested for mycoplasma contamination. Cultures were discarded after 2-3 months of use.

Transient transfection in U2OS. One day prior to transfection $4*10^5$ U2OS were seeded in a 6-wells plate. Cells were transfected by addition of a 3:1 mixture of polyethyleneimine (6 µg) and plasmid DNA (2 µg) in 200 µL serum free medium per well. The medium was refreshed after 24 hours and after 48 hours the cells were ready to be used.

***In situ* activity-based protein profiling.** Growth medium from cells grown in 6-wells plate was removed and 1 mL serum free medium containing probe **LEI-945** (1 µM, 0.1% DMSO) was added. The cells were then incubated for 1 hour. The medium was then removed, the cells were washed with 2 mL PBS and then harvested in 1 mL PBS using a cell scraper. The cells were moved to an Eppendorf tube and the suspension was centrifuged for 5 minutes at 1200 rpm. The PBS was removed and the samples snap frozen and stored at -80 °C until use.

***In situ* competitive activity-based protein profiling.** Growth medium from cells grown in 6-wells plate was removed and 1 mL serum free medium containing inhibitor or DMSO as vehicle was added (0.1% DMSO). After 1 hour of incubation 1 mL of serum free medium containing probe **LEI-945** (2 µM, 0.1% DMSO) was added. The cells were then incubated for another hour. The medium was then removed, the cells were washed with 2 mL PBS and then harvested in 1 mL PBS using a cell scraper. The cells were moved to an Eppendorf tube and the suspension was centrifuged for 5 minutes at 1200 rpm. The PBS was removed and the samples snap frozen and stored at -80 °C until further use.

CuAAC reaction and in-gel fluorescence analysis. Cell pellets were thawed on ice, lysed by addition of ice-cold lysis buffer (MilliQ, 1x protease inhibitor cocktail (Roche c*O*mplete EDTA free)) and incubated on ice (15-30 min). The protein concentration was determined by a Quick Start™ Bradford Protein assay (Bio-Rad). The protein fractions were diluted to a total protein concentration of 1 mg/mL. From each sample 40 µL was taken and treated with 5 µL from a freshly prepared "click" mixture containing 9 mM $CuSO_4$ (2.5 µL/sample, 18 mM in H_2O), 45 mM NaAsc (1.5 µL/sample, 150 mM in H_2O), 1.8 mM THPTA (0.5 µL/sample, 18 mM in DMSO) and 9 µM Alexa Fluor 647 azide (0.5 µL/sample, 90 µM in DMSO from Thermo Fischer Scientific). The samples were incubated for 1 hour at 37 °C and then 15 µL 4x SDS page sample buffer was added. The samples were denatured at 100 °C for 5 minutes. 8 µg per sample was resolved on a SDS-PAGE gel (10% acrylamide, 180 V, 75 min). Gels were visualized with a ChemiDoc XRS (Bio-Rad) using Cy3 and Cy5 multichannel settings (605/50 and 695/55, filters respectively) and stained with Coomassie or transferred to a 0.2 µm polyvinylidene difluoride membranes by Trans-Blot Turbo™ Transfer system (Bio-Rad) after scanning. Fluorescence was normalized to Coomassie staining or to FLAG-tag signal and quantified with Image Lab (Bio-Rad). IC_{50} curves were fitted with Graphpad Prism® 7 (Graphpad Software Inc.).

Western Blotting. Proteins were transferred to a 0.2 µm polyvinylidene difluoride membranes by Trans-Blot Turbo™ Transfer system (Bio-Rad). Membranes were washed with TBS (50 mM Tris, 150 mM NaCl), washed with TBS-T (50 mM Tris, 150 mM NaCl, 0.05% Tween 20) and then blocked with 5% w/v milk powder in TBS-T for 1 hour at room temperature. Membranes were then incubated with primary antibody in 5% w/v milk powder TBS-T (α-FLAG: 1 h, RT), washed three times with TBS-T, incubated with matching secondary antibody in 5% w/v milk powder TBS-T (1 h, RT) and washed with TBS-T and TBS. The blot was developed in the dark using an imaging solution (10 mL Luminol, 100 µL ECL enhancer and 3 µL 30% H_2O_2) and chemiluminescence was visualized using a ChemiDoc XRS (Bio-Rad). The signal was normalized to Coomassie staining and quantified with Image Lab (Bio-Rad). Primary antibodies: monoclonal mouse anti-FLAG (1:5000, Sigma-Aldrich, F3165). Secondary antibodies: HRP-coupled goat-anti-mouse (1:5000, Santa Cruz, sc2005).

In situ retinal conversion LC-UV/MS assay

Sample preparation. U2OS cells were grown in 6-wells plates and transiently transfected (N = 3). After 48 hours growth medium was replaces with medium containing retinal (30 µM) with serum. Cells were incubated for 4 hours, then washed with PBS and then PBS (1250 µL) was added. Cells were harvested using a cell scraper and then suspended in PBS. 1 mL of the suspension was moved to low-binding Eppendorf tube and 250 µL to a separate Eppendorf tube used to check for successful overexpression. The low-binding Eppendorf tube was spun down at 1000 g for 5 min and then PBS was removed. Samples were snap frozen and stored at -80 °C until needed. A live/dead count was performed on the cells in the remaining Eppendorf tube after which cells were lyzed using a probe sonicator (5 sec, 30%). Samples were then denatured and loaded on gel, transferred to a membrane and the overexpression visualized using anti-FLAG antibody. When required low-binding Eppendorf tubes were thawed on ice after which acetonitrile (600 µL, LC-MS grade) was added. The cells were lyzed using a probe sonicator (5 sec, 30%) and spun down (14000 g, 5 min). The lysate was transferred to a new low-binding Eppendorf tube. Lysates were collected in low-binding Eppendorf tubes, concentrated using a SpeedVac (Eppendorf) and reconstituted in LC-MS sample solution (110 µL, 90% acetonitrile). Samples were vortexed, spun down (14000 g, 5 min) and transferred (100 µL) to a LC-MS vial after which they were measured.

LC-UV/MS measurement and analysis. Samples were injected onto a C18 column (50 x 4.6 mm, 3 µm; Nucleodur Gravity, Macherey-Nagel) connected to a Vanquish UHPLC system (Thermo Scientific) with a Vanquish Diode Array detector (Thermo Scientific) coupled to a LCQ™ Fleet (Thermo Scientific) via electrospray ionisation (ESI). Acetonitrile and water containing TFA (0.1%) were used for chromatographic separate of the retinoids. The solvent gradient was run from 10% acetonitrile for 1.5 min and then increased to 90% for 7.5 min. UV spectra were recorded between 200 and 600 nm. A calibration curve was made from a mix of retinoid standards (retinol, retinal, all-*trans* retinoic acid, 9-*cis* retinoic acid and 13-*cis* retinoic acid) measured at increasing concentrations (10 nM, 25 nM, 50 nM, 100 nM, 250 nM, 500 nM, 1 µM and 2 µM; N = 2, n = 4). Samples were then measured in duplo with a washing step after each sample. Quantification was performed using Xcalibur™ software (Thermo Scientific) after which the ratio between the UV spectra selected at 324, 356 and 380 nm were calculated for each peak to determine their purity. Concentrations were calculated using the calibration curve and averaged over the two measurements. The percentages of each retinoid as part of the total amount of retinoids detected in the samples were calculated.

In situ activity-based proteomics

Sample preparation. Protocol adapted from previously described procedure.[22] Cells were treated *in situ*, harvested, lysed and adjusted to 1 mg/mL protein concentration as described above. 250 µL was taken from each sample and to this 25 µL freshly prepared "click" mixture containing 1 mM $CuSO_4$ (2.5 µL/sample, 100 mM in H_2O), 5 mM NaAsc (1.25 µL/sample, 1 M in H_2O), 0.4 mM THPTA (1 µL/sample, 100 mM in DMSO), 40 µM biotin-N_3 (2.5 µL/sample, 4 mM in DMSO) and MilliQ (17.75 µL/sample) was added. Samples were incubated for 1 hour at 37 °C while shaking (300 rpm). Excess click reagents were then removed by chloroform/methanol precipitation followed by a wash with methanol. Precipitated proteomes were then suspended in urea buffer (250 µL, 6 M urea and 25 mM ammonium bicarbonate), DTT (2.5 µL, 1M) was added and the mixture was then incubated for 15 min at 65 °C while shaking (600 rpm). The samples were then allowed to cool down to RT and then alkylated by addition of iodoacetamide (20 µL, 0.5 M) for 30 minutes at RT in the dark. Addition of SDS (70 µL, 10% (v/v)) was followed by heating at 65 °C for 5 minutes. For each sample 50 µL 50% slurry of Avidin-Agarose from egg white (Sigma-Aldrich) was washed three times with PBS and transferred in PBS (1 mL) to a 15 mL tube. To this another 2 mL of PBS was added followed by the corresponding proteome sample. The beads were incubated with the proteome for 2 hours at room temperature using an overhead shaker. The beads were then isolated by centrifugation (2 min, 2500 g), washed with SDS in PBS (0.5% (w/v)) and washed three times with PBS. The beads were then transferred to low-binding Eppendorf tubes and proteins were digested overnight at 37 °C and 950 rpm shaking in 250 µL digestion buffer (100 mM Tris, 100 mM NaCl, 1 mM $CaCl_2$, 2% acetonitrile and 0.5 µg sequencing grade trypsin (Promega)). Digestion was stopped by addition of formic acid (12.5 µL) and the beads filtered off by centrifugation (2 min, 600g) using a Bio-Spin column (Bio-Rad). Samples were then desalted using stage tips, collected in low-binding Eppendorf tubes, concentrated using a SpeedVac (Eppendorf) and stored at -20 °C until reconstitution before measurement.[23] All samples were prepared in at least three biological replicates.

LC-MS/MS measurement and analysis. Samples were reconstituted in LC-MS sample solution (50 µL, MilliQ, 3% acetonitrile/0.1% formic acid/20 fmol/µL enolase). Samples were then analysed using a NanoACQUITY UPLC System (Waters) coupled to a SYNAPT G2-Si high-definition mass spectrometer (Waters) as previously described.[22,24] Of each sample 5 µL was loaded on a nanoEASE™ M/Z Symmetry C18 trap column (particles 5 µm, 100 Å , 180 µm x 20 mm, Waters) with 0.1% formic acid and separated on an nanoEASE™ M/Z HSS C18 T3 analytical column (particles 1.8 µm, 75 µm x 250 mm, Waters) heated at 80 °C. A multistep gradient running from 5-40% acetonitrile containing 0.1% formic acid during a 70 minute method at 300 nL/min was used to achieve peptide separation. Survey scans (m/z 50-2000 Da) were acquired in the Synapt with a scan time of 0.6 seconds in positive, resolution mode. The collision energy is set to 4 V in the trap cell for low-energy MS mode. For the elevated energy scan, the transfer cell collision energy is ramped using drift-time specific collision energies. The lock mass is sampled every 30 seconds. MS raw files were analysed with ProteinLynx Global SERVER (PLGS, v3.0.3, Waters). The MS^E identification was also performed with PLGS using the human proteome from Uniprot (Uniprot-homo-sapiens-trypsin-reviewed-2016-08-29.fasta). The following parameter settings were used: low energy threshold 150 counts, elevated energy threshold 30, peptide and protein FDR 1%, enzyme specificity trypsin, max missed cleavages max 2, variable modification methionine oxidation, fixed modification carbamidomethylation cysteine, at least: fragments/peptide 2, fragments/protein 5, peptides/protein 1 and number of peptides to measure per protein 3. For label-free quantification ISOQuant (v1.5) was used.[25,26] Data were filtered to retain only proteins with two or more reported unique peptides and quantified in at least 3 replicates of the positive control (probe-treated). Proteins were designated as significantly enriched by the probe when they showed 2-fold enrichment in quantification value when comparing negative control (vehicle-treated) with positive control (probe-treated) samples, probability as determined by a Student's *t* test (<0.05) and Benjamini-Hochberg correction with an FDR of 10%. The mass spectrometry proteomics data (raw data and IsoQuant output tables for proteins groups and peptides) have been deposited in the ProteomeXchange Consortium (http://proteomecentral.proteomexchange.org) via the PRIDE partner repository with the dataset identifier PDX015495.[27,28]

Heatmap Competitive ABPP analysis. Only proteins significantly enriched were selected for analysis. Proteins were sorted on their maximal abundance. The mean raw LFQ intensities from quadruplicate measurements were normalized to DMSO (= 0) and maximal LFQ LEI-945 (= 1) for each protein individually. The heatmap was prepared using Graphpad Prism® 7 (Graphpad Software Inc.).

Supplementary Data

Supplementary Table 4.1 | Proteins significantly enriched using LEI-945 (1 µM) in A549 cells corresponding to Fig. 4.6b.

Name	Gene name	Accession	Uniprot ID	Fold change	Significance ($-\log_{10}$)
Retinol dehydrogenase 11	RDH11	Q8TC12	RDH11_HUMAN	20	2,1
Receptor expression-enhancing protein 5	REEP5	Q00765	REEP5_HUMAN	20	3,3
Peptidyl-tRNA hydrolase 2_ mitochondrial	PTRH2	Q9Y3E5	PTH2_HUMAN	20	2,1
Histidine triad nucleotide-binding protein 3	HINT3	Q9NQE9	HINT3_HUMAN	20	2,1
Cytochrome b5 type B	CYB5B	O43169	CYB5B_HUMAN	20	2,0
Transmembrane protein 245	TMEM245	Q9H330	TM245_HUMAN	20	2,6
Probable glutathione peroxidase 8	GPX8	Q8TED1	GPX8_HUMAN	20	1,9
Extended synaptotagmin-2	ESYT2	A0FGR8	ESYT2_HUMAN	20	2,5
Reticulon-3	RTN3	O95197	RTN3_HUMAN	20	2,4
Aldehyde dehydrogenase family 3 member B1	ALDH3B1	P43353	AL3B1_HUMAN	20	2,0
Fatty aldehyde dehydrogenase	ALDH3A2	P51648	AL3A2_HUMAN	16,9	2,0
Voltage-dependent anion-selective channel protein 3	VDAC3	Q9Y277	VDAC3_HUMAN	12,1	2,2
Neutral cholesterol ester hydrolase 1	NCEH1	Q6PIU2	NCEH1_HUMAN	10,8	2,2
Voltage-dependent anion-selective channel protein 2	VDAC2	P45880	VDAC2_HUMAN	8,5	2,0
Aldehyde dehydrogenase_ mitochondrial	ALDH2	P05091	ALDH2_HUMAN	6,7	2,2
Sarcoplasmic/endoplasmic reticulum calcium ATPase 2	ATP2A2	P16615	AT2A2_HUMAN	6,6	2,4
Cytoskeleton-associated protein 4	CKAP4	Q07065	CKAP4_HUMAN	5,6	2,2
PRA1 family protein 2	PRAF2	O60831	PRAF2_HUMAN	5,0	2,1
Carnitine O-palmitoyltransferase 1_ liver isoform	CPT1A	P50416	CPT1A_HUMAN	5,0	2,5
Mitochondrial carrier homolog 2	MTCH2	Q9Y6C9	MTCH2_HUMAN	4,5	4,3
Large neutral amino acids transporter small subunit 1	SLC7A5	Q01650	LAT1_HUMAN	3,3	2,3
Microsomal glutathione S-transferase 3	MGST3	O14880	MGST3_HUMAN	3,0	1,6
PCNA-interacting partner	PARPBP	Q9NWS1	PARI_HUMAN	2,7	2,4
4F2 cell-surface antigen heavy chain	SLC3A2	P08195	4F2_HUMAN	2,7	2,3
Retinal dehydrogenase 1	ALDH1A1	P00352	AL1A1_HUMAN	2,7	2,2
Dolichyl-diphosphooligosaccharide--protein glycosyltransferase subunit 2	RPN2	P04844	RPN2_HUMAN	2,7	2,1
ADP/ATP translocase 2	SLC25A5	P05141	ADT2_HUMAN	2,6	1,8
Ubiquitin-40S ribosomal protein S27a	RPS27A	P62979	RS27A_HUMAN	2,6	2,3
Transmembrane protein 33	TMEM33	P57088	TMM33_HUMAN	2,6	2,1
ADP/ATP translocase 3	SLC25A6	P12236	ADT3_HUMAN	2,4	1,9
Epoxide hydrolase 1	EPHX1	P07099	HYEP_HUMAN	2,4	1,9
Phosphate carrier protein_ mitochondrial	SLC25A3	Q00325	MPCP_HUMAN	2,3	1,9
Calnexin	CANX	P27824	CALX_HUMAN	2,2	1,9
Equilibrative nucleoside transporter 1	SLC29A1	Q99808	S29A1_HUMAN	2,2	2,9
Ras-related protein Rab-10	RAB10	P61026	RAB10_HUMAN	2,1	1,9

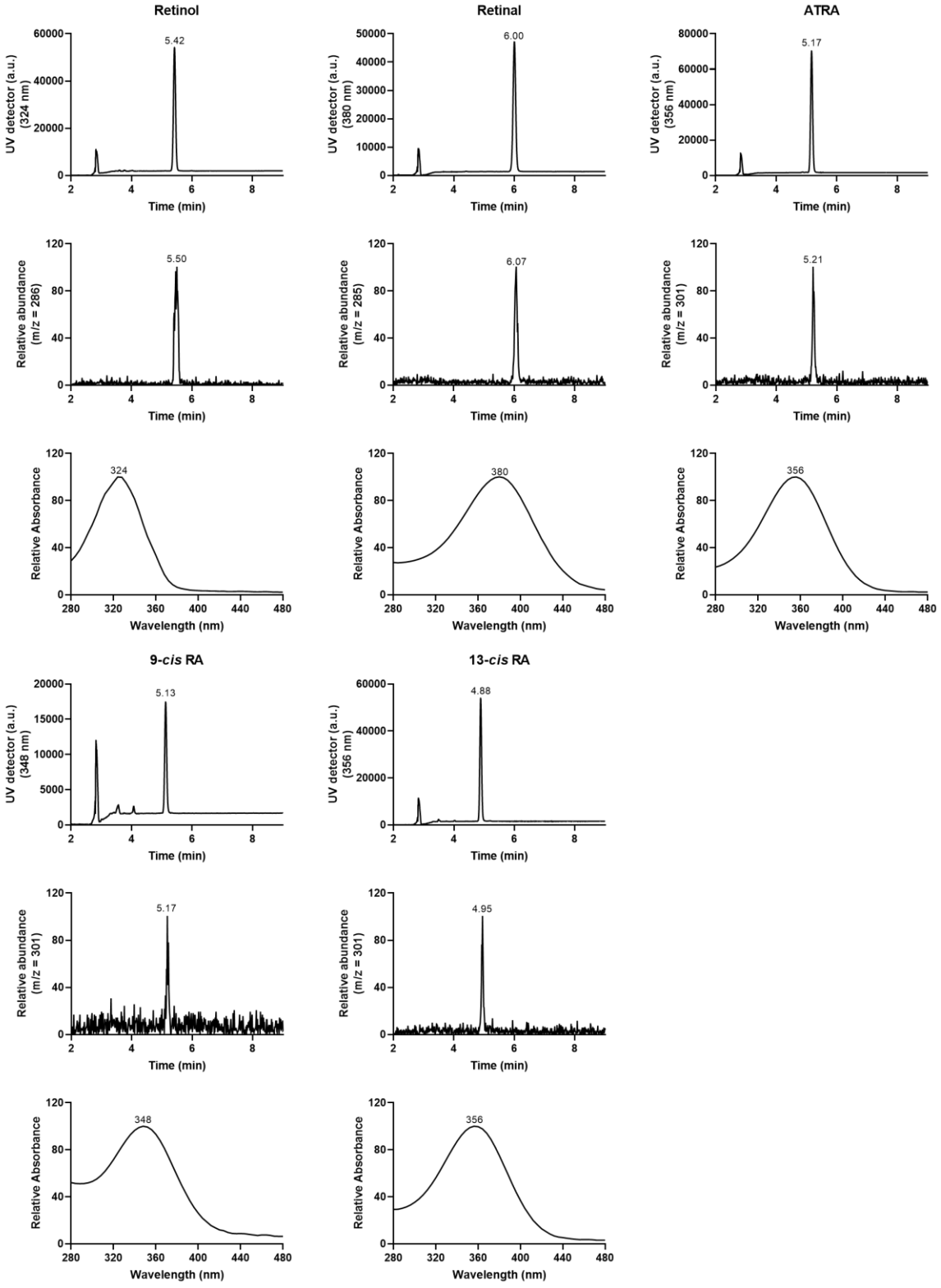

Supplementary Fig. 4.1 | LC-UV/MS spectra for retinoid standards. LC-MS traces and absorption spectra of retinoid standards used in this study. Retention time and maximum wavelength (λ_{max}) of each retinoid were determined using a gradient of 10% acetonitrile for 1.5 minutes followed by 90% acetonitrile for 7.5 minutes.

References

1. Vasiliou, V., Pappa, A. & Petersen, D. R. Role of aldehyde dehydrogenases in endogenous and xenobiotic metabolism. *Chem. Biol. Interact.* **129**, 1–19 (2000).
2. Setshedi, M., Wands, J. R. & De La Monte, S. M. Acetaldehyde adducts in alcoholic liver disease. *Oxidative Medicine and Cellular Longevity* **3**, 178–185 (2010).
3. Koppaka, V. *et al.* Aldehyde Dehydrogenase Inhibitors: a Comprehensive Review of the Pharmacology, Mechanism of Action, Substrate Specificity, and Clinical Application. *Pharmacol. Rev.* **64**, 520–539 (2012).
4. Duester, G., Mic, F. A. & Molotkov, A. Cytosolic retinoid dehydrogenases govern ubiquitous metabolism of retinol to retinaldehyde followed by tissue-specific metabolism to retinoic acid. in *Chemico-Biological Interactions* **143–144**, 201–210 (Elsevier, 2003).
5. Zile, M. H. Vitamin A and Embryonic Development: An Overview. *J. Nutr.* **128**, 455–458 (1998).
6. Wiseman, E. M., Bar-El Dadon, S. & Reifen, R. The vicious cycle of vitamin a deficiency: A review. *Crit. Rev. Food Sci. Nutr.* **57**, 3703–3714 (2017).
7. Mora, J. R., Iwata, M. & Andrian, U. H. Von. Vitamin effects on the immune system. *Nat. Rev. Immunol.* **8**, 685–698 (2008).
8. Blomhoff, H. K. *et al.* Vitamin A is a key regulator for cell growth, cytokine production, and differentiation in normal B cells. *J. Biol. Chem.* **267**, 23988–23992 (1992).
9. Kane, M. A. & Napoli, J. L. Quantification of endogenous retinoids. *Methods Mol. Biol.* **652**, 1–54 (2010).
10. Morgan, C. A., Parajuli, B., Buchman, C. D., Dria, K. & Hurley, T. D. N,N-diethylaminobenzaldehyde (DEAB) as a substrate and mechanism-based inhibitor for human ALDH isoenzymes. *Chem. Biol. Interact.* **234**, 18–28 (2015).
11. Moreb, J. S., Zucali, J. R., Ostmark, B. & Benson, N. A. Heterogeneity of aldehyde dehydrogenase expression in lung cancer cell lines is revealed by Aldefluor flow cytometry-based assay. *Cytom. Part B Clin. Cytom.* **72B**, 281–289 (2007).
12. Kang, J. H. *et al.* Aldehyde dehydrogenase is used by cancer cells for energy metabolism. *Exp. Mol. Med.* **48**, 1–13 (2016).
13. Weerapana, E. *et al.* Quantitative reactivity profiling predicts functional cysteines in proteomes. *Nature* **468**, 790–797 (2010).
14. Notario, B. All-trans-Retinoic Acid Binds to and Inhibits Adenine Nucleotide Translocase and induces Mitochondrial Permeability Transition. *Mol. Pharmacol.* **63**, 224–231 (2003).
15. Dadsena, S. *et al.* Ceramides bind VDAC2 to trigger mitochondrial apoptosis. *Nat. Commun.* **10**, (2019).
16. Budelier, M. M. *et al.* Photoaffinity labeling with cholesterol analogues precisely maps a cholesterol-binding site in voltage-dependent anion channel-1. *J. Biol. Chem.* **292**, 9294–9304 (2017).
17. Rostovtseva, T. K. & Bezrukov, S. M. VDAC regulation: Role of cytosolic proteins and mitochondrial lipids. *J. Bioenerg. Biomembr.* **40**, 163–170 (2008).
18. Ogata, H., Goto, S., Fujibuchi, W. & Kanehisa, M. Computation with the KEGG pathway database. *Biosystems* **47**, 119–128 (1998).
19. Bateman, A. UniProt: A worldwide hub of protein knowledge. *Nucleic Acids Res.* **47**, 506–515 (2019).
20. Thomas, P. D. *et al.* PANTHER: A browsable database of gene products organized by biological function, using curated protein family and subfamily classification. *Nucleic Acids Research* **31**, 334–341 (2003).
21. Huang, D. W., Sherman, B. T. & Lempicki, R. A. Systematic and integrative analysis of large gene lists using DAVID bioinformatics resources. *Nat. Protoc.* **4**, 44–57 (2009).
22. Van Rooden, E. J. *et al.* Mapping in vivo target interaction profiles of covalent inhibitors using chemical proteomics with label-free quantification. *Nat. Protoc.* **13**, 752–767 (2018).
23. Rappsilber, J., Mann, M. & Ishihama, Y. Protocol for micro-purification, enrichment, pre-fractionation and storage of peptides for proteomics using StageTips. *Nat. Protoc.* **2**, 1896–1906 (2007).
24. Distler, U., Kuharev, J., Navarro, P. & Tenzer, S. Label-free quantification in ion mobility–enhanced data-independent acquisition proteomics. *Nat. Protoc.* **11**, 795–812 (2016).
25. Distler, U. *et al.* Drift time-specific collision energies enable deep-coverage data-independent acquisition proteomics. *Nat. Methods* **11**, 167–170 (2014).
26. Kuharev, J., Navarro, P., Distler, U., Jahn, O. & Tenzer, S. In-depth evaluation of software tools for data-independent acquisition based label-free quantification. *Proteomics* **15**, 3140–3151 (2015).
27. Vizcaíno, J. A. *et al.* ProteomeXchange provides globally coordinated proteomics data submission and dissemination. *Nature*

Biotechnology **32**, 223–226 (2014).

28. Perez-Riverol, Y. *et al.* The PRIDE database and related tools and resources in 2019: Improving support for quantification data. *Nucleic Acids Res.* **47**, 442–450 (2019).